Positron lifetime spectroscopy of internally oxidised Ag-In alloys

1989 J. Phys.: Condens. Matter 1 655

(http://iopscience.iop.org/0953-8984/1/3/017)

J. Phys.: Condens. Matter **1** (1989) 655–664. Printed in the UK

Positron lifetime spectroscopy of internally oxidised Ag–In alloys

D Wegner and K P Lieb

II. Physikalisches Institut, Universität Göttingen and Sonderforschungsbereich 126, Göttingen/Clausthal, 3400 Göttingen, Federal Republic of Germany

Received 18 July 1988

Abstract. The effects of In_2O_3 precipitates on positron lifetimes after internal oxidation of α-Ag–In alloys have been investigated. A positron trap associated with the lifetime τ = 205(3) ps was detected. On the basis of the experimental results obtained for different oxidation kinetics parameters, a trapping model is proposed according to which positrons thermalised in a dislocation field around oxide precipitates are trapped at the oxide/metal phase boundary. The transition from internal to external oxidation of Ag–In was also studied. The positron lifetime in In_2O_3 was measured to be τ = 263(8) ps.

1. Introduction

Mainly in the 1960s, many experiments were performed that verified the theory of internal oxidation of binary alloys proposed by Wagner (1933, 1959); these were based on various experimental methods such as (electron) microscopy (Rapp 1961, 1965, Rapp *et al* 1964, Böhm and Kahlweit 1964), residual resistivity (Combe *et al* 1983, Ehrlich 1974), calorimetry (Charrin *et al* 1981), and tensile tests (Gregory and Smith 1956–7). When the rise of nuclear methods such as perturbed angular correlation (PAC) or Mössbauer spectroscopy offered the possibility of studying solid state reactions at a microscopic level, the field of internal oxidation processes gained new interest (Andreasen *et al* 1985, Bolse *et al* 1987, 1988, Desimoni *et al* 1983, Sanchez *et al* 1984, Wegner *et al* 1987, Niesen 1987).

In the past two decades, positron annihilation (PA) techniques have become an established tool for investigating the thermodynamics, kinetics, and nature of defects in solid state materials. For some years the technique has also been applied to two-phase systems in order to elucidate the positron-trapping mechanism of grain boundaries (McKee *et al* 1980) or the precipitation kinetics of the solute in supersaturated alloys (Lühr-Tanck *et al* 1987a, b). Theoretical work has been done treating the diffusion-limited trapping which occurs in the case of non-homogeneous distributions of trapping sites, e.g. dislocations, grain boundaries, voids, precipitates and surfaces (Brandt and Paulin 1968, 1972).

Recently, the annealing behaviour of plastically deformed silver in oxygen atmosphere and vacuum was studied via positron lifetime (PL) measurements (Wegner 1988).

0953-8984/89/030655 + 10 $02.50

Above the solubility temperature of oxygen ($T_s \simeq 470$ K), a PL component of $\tau_2 = 190(3)$ ps was found with an intensity up to 80% which, by comparison with PAC experiments, was attributed to positron annihilation in vacancies thermally stabilised by dilute impurity–oxygen molecules. The scope of the present investigation has now been extended to macroscopic internal oxides.

This work combines developments of both the internal oxidation process and the PA technique. Our motivation was to find out in which way the formation of internal oxides in a host metal influences the PA characteristics. We chose Ag–In alloys as basic material because of the high solubility of oxygen in silver (Eichenauer and Müller 1962) and the high negative formation enthalpy of indium sesqui-oxide (In_2O_3). At the oxidation front, which moves according to a parabolic time law into the volume of the alloy, oxide particles precipitate. Their average radius r depends on the distance to the surface x and the oxygen concentration c_O at the surface via

$$r = \alpha x / c_O. \tag{1}$$

The variation of α with the other thermodynamical quantities of the system has been discussed by Böhm and Kahlweit (1964).

Because the molar volume of In_2O_3 ($V_m = 38.7$ cm^3) largely exceeds that of the alloy ($V_m = 10.3$ cm^3), the formation of internal oxide causes mechanical stress which results in dislocation fields around the clusters (Combe *et al* 1983). Guruswamy *et al* (1986) have shown by optical and electron microscopy that the total volume increase by internal oxidation of AgIn leads to the formation of silver nodules free of oxide particles at the surface. The silver transport corresponds to vacancy-depleted zones around the oxide particles in the host. Taking into account the possibility of various trapping centres (e.g. oxide bulk and surface or point defects), several effects influencing the PL will have to be discussed in the interpretation of experimental data. Therefore, this work may be considered a first attempt to find out characteristic changes in PL results based on different preparation conditions. For this purpose, we conducted a number of experiments in which the oxygen pressure and the initial indium concentration were varied. Furthermore, the transition to oxide scale formation and PL in In_2O_3 powder were studied. The results will be discussed in relation to the recent work on PA in deformed and oxidised silver (Wegner 1988) and previous work on internal oxidation by other methods.

2. Experimental procedure and results

2.1. The PL spectrometer and the data treatment

All PL spectra were recorded at room temperature with a standard coincidence arrangement described elsewhere (Lühr-Tanck *et al* 1985). ^{22}Na served as the positron source. An aqueous solution of ^{22}NaCl was dropped on the disc-shaped sample and dried in Ar atmosphere. The activity of some 10^5 Bq was sandwiched between two equally prepared discs. For the PL measurements in In_2O_3, the ^{22}Na activity was sandwiched between two Ni foils 2 μm thick. With a typical count rate of 20–50 s^{-1} we accumulated spectra with 1–2 $\times$ 10^6 counts. They were fitted with the computer code POSITRONFIT EXTENDED (Kirkegaard *et al* 1981), which gave an effective time resolution of the apparatus of FWHM = 210(5) ps. The spectra were described by three lifetime components including one weak source term with intensity $I_s \simeq 5\%$ and lifetime $\tau_s \simeq 0.4(1)$ ns.

2.2. *Sample preparations and deduced PL parameters*

Stoichiometric amounts of Ag and In of 5N purity (Ventron Alfa Produkte) were melted under a protective Ar atmosphere. Surface layers of the solidified pellets were removed mechanically. Sample discs of 0.5–1 mm thickness and about 10 mm diameter were obtained by rolling. They were annealed and homogenised in evacuated quartz ampules for several days close to the respective melting temperatures.

In the following, the various oxidation treatments of the samples are described and the PL results are outlined.

2.2.1. Variation of oxygen pressure. A number of $Ag_{99}In_1$ alloys were oxidised at the temperature $T = 1175$ K under oxygen pressures $p(O_2)$ varying between 5 and 180 mbar. The duration t of the internal oxidation ($t = 16$–100 min) was chosen in such a way that the depth of the oxidation front

$$x = (4c_O D_O t/3c_{In})^{1/2} \tag{2}$$

had reached 270(10) μm in each sample (Rapp 1965). The thickness of the oxidised layer exceeds the thermalisation length (17 μm) of the incoming positrons by one order of magnitude (Linderoth *et al* 1984). Here, c_{In} denotes the indium concentration and c_O and D_O the solubility and diffusion coefficient of oxygen in silver according to Eichenauer and Müller (1962)

$$c_O = 2.12 \times 10^{-3}(p(O_2))^{1/2} \exp(-0.515\ \mathrm{eV}/k_B T) \tag{3}$$

$$D_O = 3.66 \times 10^{-3} \exp(-0.48\ \mathrm{eV}/k_B T) \tag{4}$$

where $p(O_2)$ is in mbar and D_O is in $cm^2\ s^{-1}$.

Figure 1 shows the fitted intensities I_2 and lifetimes τ_1 and τ_2 for the 1% alloys as a function of the oxygen solubility c_O according to equation (3). A lifetime component with $\tau_2 = 205(3)$ ps occurs, its intensity I_2 increasing with c_O. τ_1 is independent of I_2 and agrees with the bulk lifetime in silver $\tau_f = 130(2)$ ps (Lühr–Tanck *et al* 1985, Wegner 1987). The functional dependence between I_2 and c_O is given by

$$I_2 = ac_O/(1 + ac_O) \tag{5}$$

with $a = 2.7(4) \times 10^4$.

2.2.2. Variation of indium concentration. A series of alloys with concentration ranging from 0.2 to 2 at.% was oxidised at $T = 973$ K and $p(O_2) = 200$ mbar for $t = 5.3$ h. From these numbers oxidation depths of 220–700 μm are obtained. The evaluation of this series again yields a lifetime $\tau_2 = 205(5)$ ps, as shown in figure 2. The intensity I_2 is about 85% and is nearly independent of c_{In}. τ_1 is also close to τ_f. The almost constant intensity I_2 might be due to a saturation effect as will be discussed below.

2.2.3. Low-pressure oxidation. Another set of alloys with 0.13 at.% $\leqslant c_{In} \leqslant$ 0.81 at.% was oxidised at $T = 1173$ K and $p(O_2) \simeq 10^{-3}$ mbar for 45 h. Under these conditions, equation (2) is not valid because indium diffusion has to be taken into account ($D_O c_O \ll D_{In} c_{In}$). Indium atoms diffuse from the interior of the sample to the oxidation front. This enrichment is nicely demonstrated in figure 3, which shows an electron microanalysis of two samples oxidised under the conditions indicated in the figure. The oxidised zone is only a few micrometres thick and is not resolved within the step size (20 μm) of the analysis. Furthermore, we have to pay attention to the thermal instability of In_2O_3 under

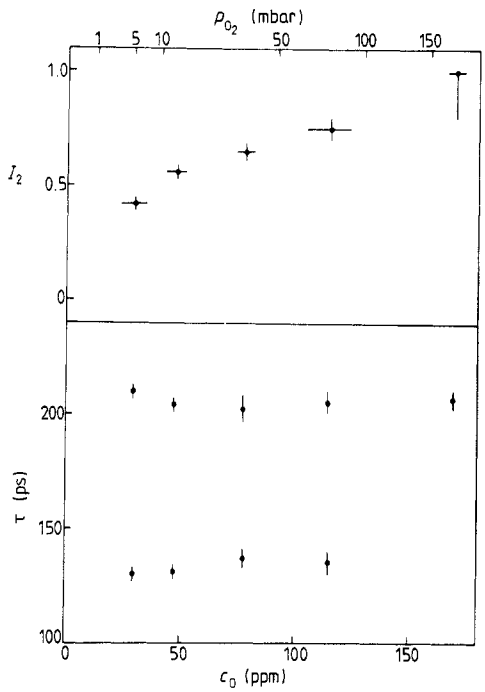

Figure 1. PL (τ_i) and intensities (I_i) as a function of the oxidation pressure WRT oxygen solubility c_O for $c_{In} = 1\%$ and oxidation temperature $T = 1173$ K.

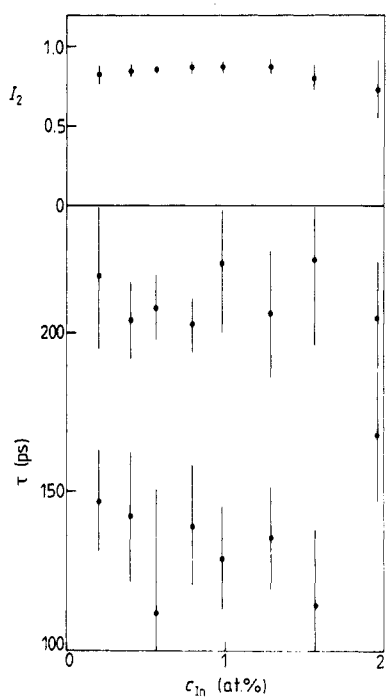

Figure 2. PL (τ_i) and intensities (I_i) as a function of c_{In} for the oxidation parameters $T = 973$ K and $p(O_2) = 200$ mbar.

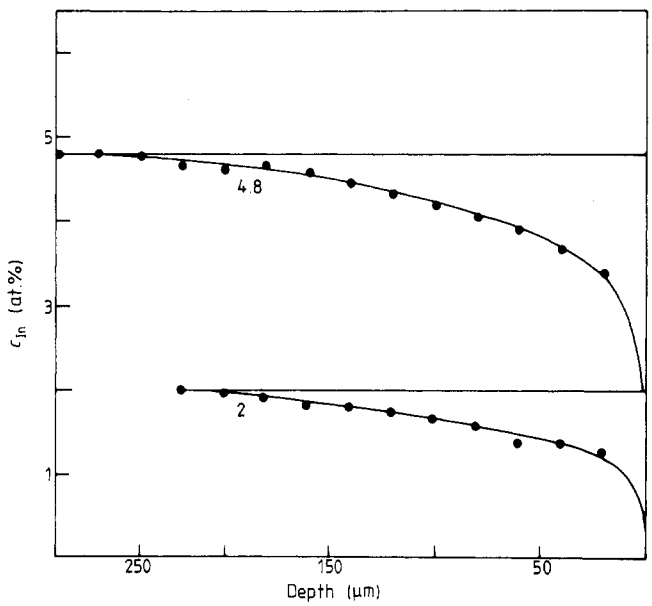

Figure 3. Electron microanalysis of two Ag–In alloys oxidised under enrichment conditions. The concentration profiles exhibit the indium depletion in front of the unresolved oxide zone. The initial indium concentrations (c^0_{In} = 2–4.8 at.%) and oxidation conditions are given by horizontal lines.

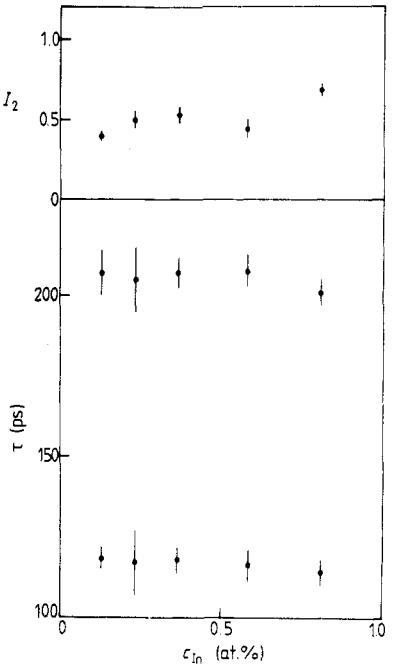

Figure 4. PL and intensities as a function of c_{In} for the oxidation parameters $T = 1173$ K and $p(O_2) = 10^{-3}$ mbar.

low oxygen pressure. This point will be discussed below. Contrary to the results of set (2), the samples oxidised at low oxygen pressure may show a slight increase of I_2 with increasing In concentration (see figure 4). While τ_2 is as before, $\tau_1 = 117(3)$ ps is less than τ_f.

2.2.4. The transition from internal to external oxidation. A series of alloys with 3 at.% $\leq c_{In} \leq 14.7$ at.% was oxidised at 973 K and 200 mbar for 3 h in order to observe the transition from internal to external oxidation due to the formation of an oxide scale, which should take place at $c_{In} \simeq 12$ at.% (Rapp *et al* 1964). The lifetimes obtained in this series for $c_{In} \geq 5$ at.% could not be determined unambiguously. Therefore, figure 5

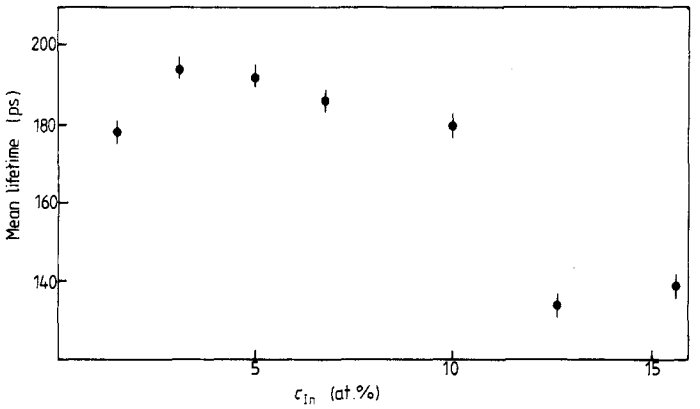

Figure 5. PL as a function of c_{In} in the internal/external oxidation transition range for $T = 973$ K and $p(O_2) = 200$ mbar.

exhibits the mean lifetime τ_m as a function of the initial In concentration. A clear drop in τ_m is visible between 10 and 12.6 at.% In.

2.2.5. PL in In_2O_3 powder. For comparison, the positron lifetime in In_2O_3 was also measured. In_2O_3 powder was pressed mechanically to various effective densities of 30–70% bulk density and dried for 1 h in a 200 mbar oxygen atmosphere at 757 K in order to avoid hydrogenation. The PL measurements yielded two components with

$$\tau_1 = 183(3)\ \text{ps} \qquad I_1 = 46(1)\%$$

and

$$\tau_2 = 420(2)\ \text{ps} \qquad I_2 = 54(1)\%.$$

These figures were independent of the average density of the powder. According to Bertolaccini *et al* (1971), if the trapping model is employed and the second component is associated with a trapped state (irrespective of its properties), one obtains $\tau_f = 263(8)$ ps for the PS bulk lifetime.

3. Discussion

The aim of the discussion is to reveal the trapped state, which is characterised by the PL $\tau_2 = 205(3)$ ps, independent of the oxidation conditions and initial alloy compositions. This constancy suggests the presence of a unique trapped positron state. By comparison of τ_2 with the results of former PL experiments (Wegner 1988), the following trapping centres can be excluded.

(i) *Oxygen-stabilised vacancies.* There is experimental evidence from this and previous work (Wegner 1988) that oxygen dissolved at 973 K with a concentration of 100 ppm in silver does not affect the PL. This can be explained by the interstitial sites of atomic oxygen in Ag and by the low concentration of oxygen–vacancy pairs at room temperature despite their considerable binding enthalpy of 0.35 eV (Combe *et al* 1983).

(ii) *Dislocations.* As mentioned in the introduction, a dense field of dislocations in the environment of the precipitates is produced. According to Wegner (1988), the PL in dislocations is $\leqslant 190$ ps, which contrasts with the present PL value.

(iii) *In_2O_3 oxide bulk.* The measured bulk PL in In_2O_3, $\tau = 263(8)$ ps, is consistent with the empirical relation between the effective anion density and the annihilation rate found by Bertolaccini *et al* (1971) for ionic media. The PL differs significantly from the τ_2-value obtained for the internally oxidised alloys.

(iv) *Oxide molecule stabilised vacancies.* After annealing plastically deformed silver in oxygen atmosphere, a trapped positron state with $\tau = 190(3)$ ps was observed. It was tentatively associated with the formation of impurity oxide vacancy complexes (Wegner 1988). The value of τ is equal to the PL in monovacancies in silver and different from the τ_2-value of the present experiments. Furthermore, PAC experiments have shown that In–oxygen vacancy complexes dissociate above 800 K (Schröder *et al* 1986, Wegner *et al* 1987).

When we had excluded the foregoing traps, we were led to the following hypothesis: the positrons in internally oxidised Ag–In alloys are trapped at the surfaces of the In_2O_3 precipitates. In_2O_3 is known as an n-type semiconductor (Hamberg and Granqvist 1986). Due to the oxygen deficiency found in PAC experiments (Desimoni *et al* 1983), the donor

concentration of internal oxide precipitates ought to be considerably larger than that in stoichiometric In_2O_3. The oxide–metal interface either forms a Schottky contact or an Ohmic junction, according to the electron work functions of the components. The ^{111}Cd hole recovery rate in internal In_2O_3 in Ag was measured via the PAC technique by Massolo *et al* (1986). These experiments revealed that the rate of the electron–Cd hole recombination process increases with decreasing oxide precipitate size. The effect was explained with an Ohmic semiconductor–metal contact, which increases the electron availability at the Cd impurity sites located in the contact zone of the oxide. The charge distribution and electronic potential in the contact region are sketched in figure 6. The figure indicates that the oxide surface can act as a positron trap. The hypothesis suggests that the measured τ_2-value ranges between the Ag and In_2O_3 bulk values. According to Guruswamy *et al* (1986), the growing oxide particles lead to high dislocation densities via deformation of the surrounding silver lattice. This effect is visible in a stress- and dislocation-induced broadening of x-ray diffraction patterns. Figure 7 shows, for comparison, the (331) and (420) reflections of pure Ag and a 5 at.% Ag–In alloy oxidised at 973 K and 200 mbar (Schröder 1985). The peak width has increased by a factor of 3. The flow of superceded silver atoms takes place via dislocation pipe diffusion from the precipitate surfaces to grain boundaries and to the sample surface. The dislocation density was estimated to be of the order of 10^{11} cm^{-2}.

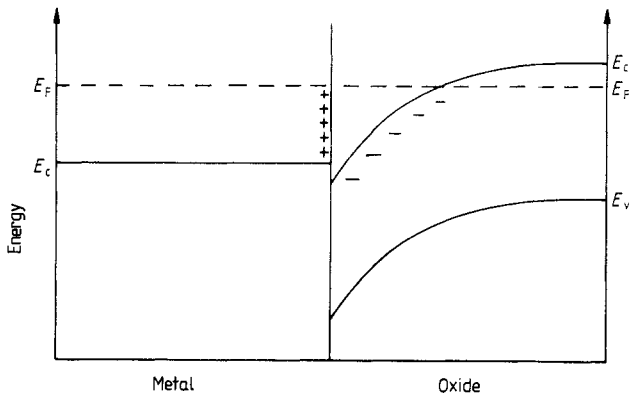

Figure 6. Sketch of the electronic potential and charge distribution at an Ohmic metal/*n*-semiconductor contact.

From this scenario, we arrive at the following trapping mechanism for positrons. Each precipitate is surrounded by a dense dislocation field. Its volume is assumed to be proportional to the particle surface. Then the total volume is proportional to $Z(x)A(x)$, where $Z(x)$ and $A(x)$ are the number of precipitates per volume WRT their surface, and is therefore dependent on the distance x to the sample surface. The simplest idea of a two-state trapping model which accounts for the inhomogeneity of the system, supposes a positron to be thermalised either in the undisturbed silver bulk or in a dislocation field near a precipitate surface. We are, of course, aware of the fact that a more realistic trapping model should explicitly account for inhomogeneity, positron diffusion and a greater number of positron states (≥ 3)). However, the proposed simple scheme accounts for the following observations.

(i) In all experiments, we found $\tau_1 \simeq \tau_f$, i.e. the trapping rate κ for positrons in the

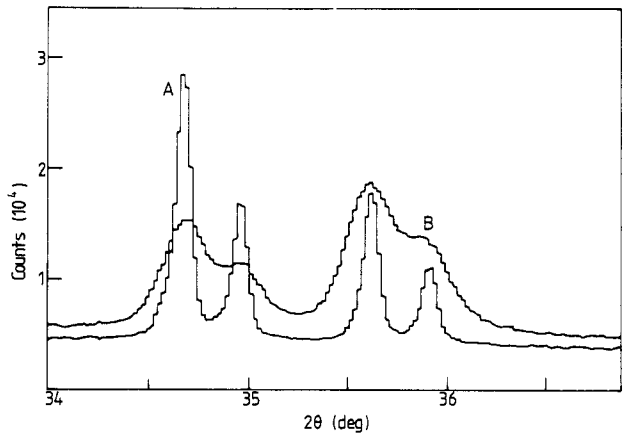

Figure 7. X-ray diffraction intensities of the (331) and (420) planes of pure polycrystalline Ag (curve A) and a 5% AgIn alloy oxidised at 973 K and $p(O_2) = 200$ mbar (Cu $K\alpha_1$ and $K\alpha_2$ lines) (curve B).

silver bulk is small. In case of homogeneously distributed traps one could have expected the relation $I_1\lambda_1 = \lambda_f - I_2\lambda_2$, which is not fulfilled in the present case.

(ii) In experiment 1 (variation of oxygen pressure), I_2/I_1 is proportional to c_O. According to Böhm and Kahlweit (1964), $Z(x)$ and $A(x)$ vary as $(c_O/x)^3$ WRT $(x/c_O)^2$, thus $Z(x)A(x) \simeq c_O/x$. Even if Ostwald ripening plays a role, this proportionality is still valid (Böhm and Kahlweit 1964).

(iii) In experiment 2, saturated trapping occurred. Experimental observations show that the size of precipitates grows with increasing temperature WRT decreasing $c_O D_O/D_{In}$ (Combe *et al* 1983, Charrin *et al* 1981, Gregory and Smith 1956–7). Assuming a linear scaling of $Z(x)A(x)$ with $c_O D_O/D_{In}$, we find that $Z(x)A(x)$ in experiment 2 is larger by a factor 4.6 than in experiment 1. The intensity I_1 is traced to positron annihilation in silver nodules set on the sample surface. A uniform layer of the out-diffused silver atoms would yield I_1-values ranging between 7% ($c_{In} = 0.2$ at.%) and 19% ($c_{In} = 2$ at.%) where the fraction of thermalised positrons was calculated according to Linderoth *et al* (1984).

(iv) In experiment 3 (variation of In concentration), I_2/I_1 increases approximately as $c_{In}^{2/3}$. Up to now no calculation for the scaling of $Z(x)$ exists which accounts for indium enrichment. Nevertheless, extrapolations of the theoretical (Böhm and Kahlweit 1964, Ehrlich 1974) or experimental results (Massolo *et al* 1986) to the present situation agree with the trend observed here. In particular, it is to be noted that τ_1 deviates from τ_f in this series. In the standard trapping model the difference would correspond to an intensity $I_2 = 23\%$, which is below the measured value $I_2 \simeq 50\%$. We suggest that here the usually employed mechanism of internal oxidation providing irreversible precipitation of oxide fails. From PAC experiments (Schröder *et al* 1986), it is known that InO_x molecules in Ag, i.e. the precipitate 'embryos', dissociate in a vacuum of 10^{-5} mbar at 1000 K. From the free enthalpy of the reaction $2\,In + \frac{3}{2}O_2 \rightarrow In_2O_3$, $\Delta G = -3.13 + 1.24eVT/1000$ (where T is in K) (Raub 1976), the stability limit of In_2O_3 at 1173 K is estimated at $p(O_2) \simeq 10^{-2}$ mbar. Therefore, we assume that during the oxidation substitutional In, interstitial oxygen, oxide molecules and oxide precipitates are in equilibrium.During the slow cooling down of the oxidised samples, precipitates form from this mixture. Nevertheless, neither oxidation nor precipitation are complete and a

considerable fraction of homogeneously distributed small precipitates may account for the observed trapping effect with the consequence $\tau_1 < \tau_f$. According to Wegner (1987), we can exclude the hypothesis that the low-concentrated substitutional In in Ag plays a significant role. The assumption that the low-pressure oxidation mechanism differs from the basic theory in principle explains that the results of series (3) do not fit into the systematics of experiment (1), which predict by extrapolation $I_2 = 0$ for $p(O_2) \rightarrow 0$.

(v) The validity of the proposed trapping model is limited to dispersed internal oxide particles. Therefore it cannot work in the case of indium concentrations around 10 at.% corresponding to at least 20% oxide volume fraction. In the considered concentration range 'large' precipitates are expected, which occupy (via indium enrichment and oxygen blocking) some 10% of the total volume. This explains why a two-component fit of the the lifetime spectra obtained in experiment 4 gave lifetimes that did not change in a systematic manner. Nevertheless, the transition to external oxidation is clearly visible. The drop in the mean lifetime is due to the fact that the In_2O_3 layer prevents internal oxidation. The thickness of this In_2O_3 oxide scale is of the order of several micrometres.

4. Summary

The positron lifetimes in internally oxidised Ag–In alloys have been measured. A long lifetime $\tau_2 = 205(3)$ ps was traced to annihilation at an internal oxide surface that acts as a positron trap due to the Ohmic Ag/In_2O_3 junction. τ_2 lies in between the bulk lifetimes of pure Ag ($\tau = 130(1)$ ps) and In_2O_3 ($\tau = 263(8)$ ps). A naive trapping model is proposed according to which only positrons thermalised in the dense dislocation field around precipitates are trapped. The model accounts for all experimental observations, including extreme cases, as transition to external oxidation and oxidation at high temperature and low pressure. It could be checked and improved by depth-sensitive analyses (positron beams or lapping) in combination with microstructural analysis.

Acknowledgments

We are indebted to Professor Th Hehenkamp and Dr W Lühr-Tanck for letting us use their lifetime spectrometer. We gratefully acknowledge the help of Th Kurschat and A Sager during the experiments and analysis. Some of the calculations were performed at the UNIVAC computer of the Gesellschaft für wissenschaftliche Datenverarbeitung Göttingen.

References

Andreasen H 1985 *Hyperfine Interact.* **23** 43–63
Bertolaccini M, Bisi A, Gambarini G and Zappa L 1971 *J. Phys. C: Solid State Phys.* **4** 734
Böhm G and Kahlweit M 1964 *Acta Metall.* **12** 641
Bolse W, Lieb K P, Uhrmacher M and Wegner D 1988 in *XXV Escuela Latinoamericana de Fisica* (Singapore: World Science) at press
Bolse W, Uhrmacher M and Lieb K P 1987 *Phys. Rev.* B **36** 1818–30
Brandt W and Paulin R 1968 *Phys. Rev. Lett.* **21** 193–5
—— 1972 *Phys. Rev.* B **5** 2430–5
Charrin L, Combe A and Moya G 1981 *Acta Metall.* **29** 1593–8
Combe A, Charrin L, Moya G and Cabane J 1983 *Acta Metall.* **31** 1019–23

Desimoni J, Bibiloni A G, Mendoza-Zélis L, Pasquevich A F, Sanchez F H and Lopez-Garcia A 1983 *Phys. Rev.* B **28** 5739–45
Ehrlich A C 1974 *J. Mater. Sci.* **9** 1064–72
Eichenauer W and Müller G 1962 *Z. Metall.* **53** 321
Gregory E and Smith G C 1956–7 *J. Inst. Met.* **85** 81–7
Guruswamy S, Park S M, Hirth J P and Rapp R A 1986 *Oxid. Met.* **26** 77–100
Hamberg I and Granqvist C G 1986 *J. Appl. Phys.* **60** R123–59
Kirkegaard P, Eldrup M E, Mogensen D E and Petersen N J 1981 *Comput. Phys. Commun.* **23** 307
Linderoth S, Hansen H E, Nielsen B and Petersen K 1984 *Appl. Phys.* A **33** 25
Lühr-Tanck W, Kurschat T and Hehenkamp T 1985 *Phys. Rev.* B **31** 6994
Lühr-Tanck W, Sager A and Bosse H 1987a *J. Phys. F: Met. Phys.* **17** 827–36
Lühr-Tanck W, Sager A, Ederhof M and Bosse H 1987b *Phys. Status Solidi* a **102** 133–8
Massolo C P, Desimoni J, Bibiloni A G, Mendoza-Zélis L A, Sanchez F H, Pasquevich A F and Lopez-Garcia A R 1986 *Hyperfine Interact.* **30** 1–8
McKee B T A, Carpenter G J C, Watters J F and Schultz R J 1980 *Phil. Mag.* A **41** 65–80
Niesen L 1987 *Hyperfine Interact.* **35** 587
Rapp R A 1961 *Acta Metall.* **9** 730
—— 1965 *Corrosion* **21** 382
Rapp R A, Frank D F and Armitage J V 1964 *Acta Metall.* **12** 505
Raub E 1976 *Gase und Kohlenstoff in Metallen* ed. E Fromm (Berlin: Springer) p 678
Sanchez F H, Mercader R C, Pasquevich A F, Bibiloni A G and Lopez-Garcia A 1984 *Hyperfine Interact.* **20** 295–303
Schröder H 1985 *PhD Thesis* University of Götttingen
Schröder H, Bolse W, Uhrmacher M, Wodniecki P and Lieb K P 1986 *Z. Phys.* B **65** 193
Wagner C 1933 *Phys. Chem.* B **21** 25
—— 1959 *Z. Elektrochem.* **63** 1772
Wegner D 1987 *J. Phys. F: Met. Phys.* **17** L289
—— 1988 *J. Phys. F: Met. Phys.* **18** 2291–302
Wegner D, Uhrmacher M and Lieb K P 1987 *Z. Phys.* B **68** 461